Receiver Bandwidth Effect on Reflectivity and Doppler Velocity Estimates

R. J. DOVIAK AND DUSAN ZRNIC'

NOAA, National Severe Storms Laboratory, Norman, OK 73064

(Manuscript received 14 June 1978, in final form 7 September 1978)

ABSTRACT

Probert-Jones' radar equation assumes receiver bandwidth large compared to the reciprocal of the transmitted pulse width τ. The advent of coherent radars with precise transmitter frequencies allows consideration of receiver bandwidth "matched" to and sometimes smaller than τ^{-1} in order to enhance measurement signal-to-noise ratio.

An extension to the radar equation has been made to show explicitly the dependence of echo power on the product of transmitter pulse width and receiver bandwidth. When receiver bandwidth is less than twice τ^{-1}, there is significant loss in echo power. This should be accounted for when estimating reflectivities.

Considerable improvement in Doppler velocity estimation can often be obtained by matching range resolution to the angular one and this has implications of practical importance when moderately sensitive dual-Doppler radars are used to map the mesoscale wind in clear air.

1. Introduction

Probert-Jones (1962) developed a now widely accepted weather radar equation. However, he did not take into account echo power loss related to bandwidth and thus implicitly assumed bandwidth large compared to the reciprocal of the transmitted pulse width τ.

Loss in weather echo signal strength due to finite receiver bandwidth was first enunciated by Nathanson and Smith (1972) to explain certain discrepancies between measurements and theory. Probert-Jones' expression applies whenever the bandwidth is much larger than τ^{-1}, a condition often found in many incoherent weather radar systems. However, wide receiver bandwidths result in detection performance less than optimum. Zrnic' and Doviak (1978) have developed matched filter design criteria that optimize weather echo signal-to-noise power given a required range resolution. Optimization of signal detection plays an important role in the detection of clear-air echoes with moderate power weather radar systems (Hennington *et al.*, 1976).

Now Doppler radars use very stable oscillators so that bandwidths can be adjusted to optimize signal detection performance without worry that signals will fall outside the passband frequencies. However, optimization causes receiver bandwidth loss that should be part of the weather radar equation as are other losses such as atmospheric attenuation (Atlas, 1964). Furthermore, finite bandwidth receivers cause spatial weighting along the range-time axis just as important as the antenna pattern weighting along angular directions.

Calibration of the radar receiver with pulses of duration equivalent to that transmitted does not lend itself to easy determination of weather echo losses due to finite receiver bandwidth—it is not simply the ratio of the peak output to the input amplitude. Calibration with cw signals, although convenient because all range bins of an echo power processor can be calibrated simultaneously, also fails to account for receiver bandwidth loss. Therefore, we here develop an extension of Probert-Jones' equation to show explicitly how echo power depends on the product of transmitter pulse width and receiver bandwidth.

2. Filtered waveform

Before developing the radar equation for a distribution of point scatterers, we first consider this equation for a point target for which the echo $V_i(t)$ at the receiver input replicates the rectangular transmitted pulse. We then examine the output waveform $V_0(t)$ after the echo passes through a filter of finite bandwidth.

The echo output waveform $V_0(t)$ is the convolution of the filter's impulse response $h(t)$ with the echo input pulse waveform, i.e.,

$$V_0(t)=\int V_i(\alpha)h(t-\alpha)d\alpha. \tag{1}$$

Quite often the passband frequency (f) response of synchronously tuned intermediate frequency amplifiers can be well approximated by a Gaussian function

(Taylor and Mattern, 1970). Consider the response

$$G(f)=\exp[-(4\ln 2)f^2/B_6^2], \quad (2)$$

where B_6 is the 6 dB filter bandwidth. This filter's unit impulse response is

$$h(t)=(\pi/4\ln 2)^{\frac{1}{2}}B_6\exp[-(\pi B_6 t)^2/4\ln 2]. \quad (3)$$

Substituting (3) into (1) and performing the indicated integration we obtain the output echo wave form

$$V_0(t)=\tfrac{1}{2}A_0\{\mathrm{erf}[aB_6(t+\tau/2)]-\mathrm{erf}[aB_6(t-\tau/2)]\}, \quad (4)$$

where A_0 is the prefilter echo amplitude $a=\pi/2\sqrt{\ln 2}$, erf [ ] is the error function (Abramowitz and Stegun, 1964) and $t=0$ is the time at which $V_0(t)$ is maximum. Although (4) approximates the pulse shape if the actual filter response is well represented by (2), it has the defect of producing signal for all t—it does not show a starting time. This is because the actual frequency response approaches Gaussian only with the concurrent limit of an infinite propagation delay through the filter. Nevertheless, the Gaussian approximations are excellent around the peak responses although poor at the tails and (4) is instructive because it shows the interrelation between B_6, τ and range-time τ_s (we relate τ_s to t in Section 4). Range-time is the delay measured relative to the time a pulse is transmitted. It can readily be seen from substitution into (4) that when B_6 is much larger than τ^{-1}, the filtered echo pulse is a scaled replica of the transmitted pulse.

The filter bandwidth and shape, important to the radar meteorologist, specify the range weight given to samples of echoes from distributed targets such as rain. Often B_6 is chosen significantly larger than that required to produce an acceptable echo response in order to allow for frequency instabilities in incoherent radar transmitters. A filter can also reject interference from extraneous sources and smaller B_6 makes the receiver more selective. A rectangular filter shape is much more frequency selective than the Gaussian filter but its time response to echo pulses may be objectionable because of larger reverberating signals—these mask nearby weak echoes and, in rainshowers, smear gradients of rain intensity. A Gaussian filter is often a good compromise between frequency selectivity and a time response having echo power quickly decaying after the peak.

3. Signal-to-noise ratio, matched filter

An important specification in radar performance is the peak signal power-to-noise power ratio. The peak signal power S is readily obtained from the above equations and noise power N is

$$N=kT_eB_n, \quad (5)$$

where k is the Boltzmann's constant ($k=1.38\times10^{-23}$ W s K^{-1}), B_n the filter's noise bandwidth and T_e the effective temperature at the receiver's front end. It is referred to as the system temperature which includes contribution from environmental noise received via the antenna, thermal radiation due to losses in the transmission line, and protective radome as well as thermal noise within the receiver itself (Blake, 1970, pp. 2–29).

Thus the peak signal-to-noise ratio S/N is

$$\frac{S}{N}=\frac{A_0^2\,\mathrm{erf}^2[aB_6\tau/2]}{kT_eB_n}. \quad (6)$$

We have omitted a constant impedance factor which needs to be incorporated into (6) to make it dimensionally correct. But here we are only interested in the values of B_6, τ that maximize (6). For Gaussian filter shape and white noise $B_n=1.06\,B_6/\sqrt{2}$ and from (6) we find that S/N is maximized when

$$B_6=1.04/\tau. \quad (7)$$

Taylor and Mattern (1970, pp. 5–25) show that for a wide variety of filter responses Eq. (7) optimizes the S/N and for our purposes is considered to "match" the filter.

It is well known that S/N is maximized when the filter response is matched to the prefilter echo spectrum (see, e.g., Nathanson, 1969, p. 277). The Gaussian filter therefore does not match the spectrum of our rectangular transmitted pulse. But to simplify the filter hardware, a matched filter is often only approximated in practice.

4. Weather echo signals

The previous section has delineated, for linear receivers, the radar signal properties of echoes from discrete targets having dimensions considerably smaller than the spatial pulse width $C\tau$. Weather echoes are a composite of signals from a very large number of such discrete targets collectively designated as distributed targets or clutter. We do not resolve individual targets but sample instantaneously the composite echo at discrete range-time delays τ_s (Fig. 1). Samples at fixed τ_s taken at T_s intervals are used to construct a Doppler spectrum for scatterers located about the range $C\tau_s/2$.

Each sample is a composite of discrete echoes from all the scatterers each having a weight determined by the normalized radiation pattern $f^4(\theta,\phi)$ as shown by Probert-Jones (*op. cit.*) and, as will be shown here, the receiver bandwidth-transmitted pulse duration product $B_6\tau$ (θ, ϕ are the target's angular position relative to the main beam axis). These weighting functions determine a resolution volume in space wherein targets significantly contribute to the echo sample at τ_s.

Thus the weather echo sample $V(\tau_s)$ is

$$V(\tau_s)=\sum_i A_iW_ie^{j4\pi r_i/\lambda}, \quad (8)$$

where A_i is the prefilter echo amplitude of the ith scatterer located at r_i and $W_i=W(\tau_s-2r_i/C)$ is the filter output response. The summation includes contributions from all targets but, because of W, some are weighted more than others. Furthermore, the antenna weighting factor $f^4(\theta,\phi)$ is assumed part of A_i. We also assume target velocity to be sufficiently small so that W_i is independent of it (i.e., the Doppler shift is small compared to B_6). Although we can use (4) as a realistic weighting function, we need to incorporate into it a time delay τ_r, the delay between arrival of the echo at the receiver and the peak of W (Fig. 2). The time delay τ_r is a quantity that is best measured and can include other delays in the radar system. Real receivers produce $W(\tau_s)=0$ for $\tau_s \leqslant 2r_i/C$ and therefore Eq. (4) approximates the true response about the $W(t)$ peak. Because $W(t)$ decays rapidly for large arguments, insignificant weight is given to targets far removed from those principally weighted. Consequently, we can assume the cross section of each scatterer to have a range-dependent weight

$$W_i=\tfrac{1}{2}\{\mathrm{erf}[aB_6(\tau_s-\tau_r-2r_i/C+\tau/2)] - \mathrm{erf}[aB_6(\tau_s-\tau_r-2r_i/C-\tau/2)]\} \quad (9)$$

for the sample taken at delay τ_s. When scatterers are nearly identical, the ones which contribute most to the echo sample at τ_s have range

$$r_i=C(\tau_s-\tau_r)/2. \quad (10)$$

The echo sample power is proportional to

$$P(\tau_s) \propto \tfrac{1}{2}[VV^*]=\tfrac{1}{2}\sum_{i,k}^{N_s} A_iA_kW_iW_k^*e^{j4\pi(r_i-r_k)/\lambda} \propto \tfrac{1}{2}\sum_{i}^{N_s} A_i^2W_i^2+\tfrac{1}{2}\sum_{i\neq k}^{N_s} A_iA_kW_iW_k^*e^{j4\pi(r_i-r_k)/\lambda}, \quad (11)$$

where the asterisk signifies the complex conjugate. The above is the instantaneous echo power $P(\tau_s)$ for one transmission and N_s is the number of scatterers.

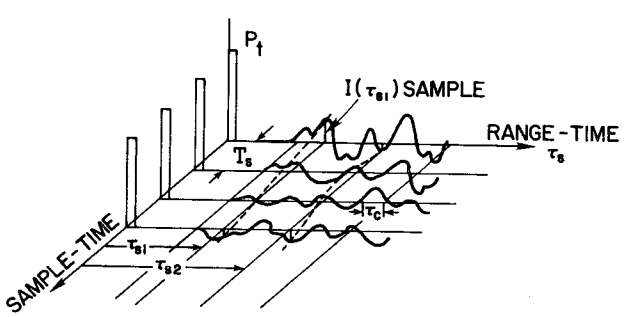

FIG. 1. Idealized traces of echoes from distributed targets for a Doppler receiver. Each trace represents echoes from a single transmitted pulse P_t. Instantaneous samples are taken at τ_{s1}, τ_{s2}, etc. Dashed line indicates probable time dependence of the in-phase component $I(\tau_s)$ sample at τ_s. τ_c depicts signal correlation time along τ_s and is related to $B_6\tau$.

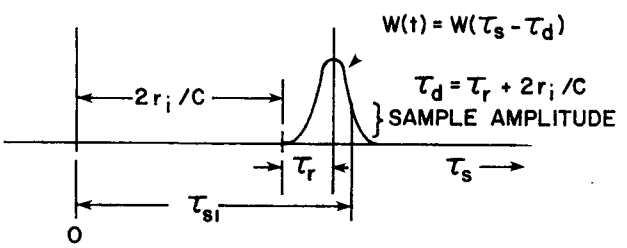

FIG. 2. Realistic receiver response to point target echo of a rectangular transmitter pulse. Time delays relate to target range r_i, receiver response delay τ_r and sample delay τ_{s1}.

Although the second sum can be significantly larger than the first [it has $N_s(N_s-1)$ contributions compared to N_s for the first term] for some echo samples at the same τ_s, its average over many successive samples (i.e., sample-time average) approaches zero for spatially uniform scatterer distributions because the average of the exponential term tends to zero. The first sum is then the mean power $\bar{P}(\tau_s)$ of the echo sample. An accurate estimate of this term is important because it relates to the liquid water content in the sample volume.

5. The weather radar equation

We are now in a position to relate the average power $\bar{P}(\tau_s)$ to the radar parameters and target cross section. The contribution to $P(\tau_s)$ from each scatterer is

$$P_i=\tfrac{1}{2}A_i^2W_i^2, \quad (12)$$

where $A_i^2/2$ is the pre-filter echo power P_{ri}, and hence can be directly expressed in terms of radar parameters and target cross section through use of the radar equation for point target scatterers:

$$P_{ri}=\frac{P_tg^2\lambda^2l_i^2\sigma_{bi}f^4(\theta,\phi)}{(4\pi)^3r_i^4}, \quad (13)$$

where l_i^2 is the two-way atmospheric loss factor, σ_{bi} the backscatter cross section of the ith scatterer at range r_i and g the antenna gain along the main beam axis. Gain g should be a measured value because it can include losses that are difficult to measure separately (e.g., radome, spillover, blockage losses, etc.).

Thus the sample-time average power at delay $\tau_s=2r/C$ is

$$\bar{P}(\tau_s)=\frac{P_tg^2\lambda^2}{(4\pi)^3}\sum_i \frac{l_i^2\sigma_{bi}f^4(\theta_i,\phi_i)W_i^2}{r_i^4}. \quad (14)$$

Replacing the sum by an integration because hydrometeors are usually closely spaced compared to the scale of the weighting functions and recalling that reflectivity (the scatter cross section per unit volume) is

$$\eta=(\Delta V)^{-1}\sum_{\Delta V}\sigma_{bi}, \quad (15)$$

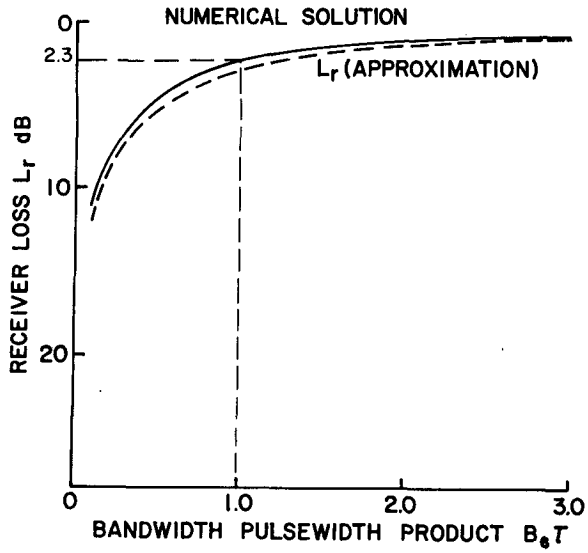

FIG. 3. Receiver signal power loss L_r(dB) due to finite bandwidth. Receiver frequency transfer is Gaussian and transmitted pulse rectangular. The solid curve is a numerical solution of the exact response function and the dashed curve is obtained from an analytic approximation [Eq. (21)].

we obtain the weather radar equation

$$\bar{P}(\tau_s)=\frac{P_t g^2\lambda^2}{(4\pi)^3}\int_V \frac{\eta(\theta,\phi,r)l^2(r)}{r^4} \times f^4(\theta,\phi)W^2(\tau_s-\tau_d)dV, \quad (16)$$

where $dV=r^2dr\cdot\sin\theta d\theta d\phi$. W is dependent on r because $\tau_d=\tau_r+2r/C$. In general, η,l are functions of r, θ, ϕ, but we assume that $f^4(\theta,\phi)W^2(r)$ has a scale (resolution volume dimensions) such that the reflectivity and attenuation can be considered constant over the region which contributes most to $\bar{P}(\tau_s)$ and that insignificant contribution comes from regions outside the resolution volume. The assumption that reflectivity does not change within the resolution volume is not always valid, but this greatly simplifies the formulas while retaining most of the physical insight. We also assume range to resolution volume large compared to its range extent. We shall be more precise in our definition of resolution volume size in Section 6. Thus we approximate (16) by

$$\bar{P}(\tau_s)\approx\frac{P_t g^2\lambda^2 l^2\eta}{(4\pi)^3 r^2}\int_0^\infty W^2(r)dr \times\int_0^{2\pi}\int_0^{\pi} f^4(\theta,\phi)\sin\theta d\theta d\phi. \quad (17)$$

When antenna patterns are circularly symmetric and with Gaussian shape Probert-Jones (1962) showed that

$$\int\int f^4(\theta,\phi)\sin\theta d\theta d\phi=\frac{\pi\phi_1^2}{8\ln 2}, \quad (18)$$

where ϕ_1 is the 3 dB width of the one-way pattern.

We express the range weighting function $W(r)$ as a product of a receiver loss factor l_0 and a weighting function $f_w(r)$ whose peak is normalized to unity in order to have a form analogous to the product of antenna gain g and power pattern function $f^2(\theta,\phi)$. We define

$$\int W^2(r)dr=\int l_0^2 f_w^2(\tau_s,r)dr\equiv l_r C\tau/2, \quad (19)$$

where l_r is the echo power loss due to finite receiver bandwidth.

For Gaussian frequency transfer

$$l_0=\mathrm{erf}(b), \quad (20a)$$

$$f_w(\tau_s,r)=\frac{1}{2\,\mathrm{erf}b}\{\mathrm{erf}(x+b)-\mathrm{erf}(x-b)\}, \quad (20b)$$

$$b=aB_6\tau/2; \quad a=\pi/2\sqrt{\ln 2}, \quad (20c)$$

$$x=(\tau_s-\tau_r)aB_6-2aB_6r/C. \quad (20d)$$

By approximating erf[ ] with tanh [ ], we obtain an analytic solution to l_r

$$l_r=[(\coth 2b)-1/2b]. \quad (21)$$

The receiver loss $L_r=-10\log l_r$ is plotted in Fig. 3 along with a numerical solution of (19). From this figure we see that if $B_6\tau>1$ the approximation formula (21) has an error less than 0.6 dB. However, for $B_6\tau<1$ we need the exact solution for accurate calibration. In the limit $B_6\tau\ll 1$, the loss of signal power due to finite receiver bandwidth is

$$L_r\to -10\log(aB_6\tau/3). \quad (22)$$

Thus we see that echo sample power decreases linearly with B_6 for $B_6\tau\ll 1$. This may seem disastrous but what really counts is the desired spatial resolution and signal-to-noise ratio. These influence the variance of measured meteorological parameters. Furthermore, we note that for $B_6\tau\ll 1$, $l_r\to 1$, $\int W^2dr\to C\tau/2$ and the weather radar equation (17) agrees with that of Probert-Jones.

Incorporating (18)–(21) into (17) yields

$$\bar{P}(\tau_s)=\frac{P_t g^2\lambda^2 l^2\eta}{(4\pi)^3 r^2}[\coth(\pi B_6\tau/2\sqrt{\ln 2})-(\pi B_6\tau/2\sqrt{\ln 2})^{-1}] \times\frac{\pi\phi_1^2}{8\ln 2}\frac{C\tau}{2}. \quad (23)$$

This extended weather radar equation shows not only the dependency of $\bar{P}(\tau_s)$ upon commonly used parameters measured for the radar but also its relation to receiver bandwidth. For radar receivers having B_6 nearly equal to or less than τ^{-1}, l_r is significant (for "matched" filter receiver, $L_r=2.3$ dB) and needs to be accounted for in the weather radar equation.

6. The resolution volume

For many reasons it might be useful to define the resolution volume as that enclosed by the 6 dB contour. The 6 dB width of $f^4(\theta,\phi)$ (corresponding to the 3 dB one-way antenna pattern width) can represent the angular extent of the resolution volume. In an analogous manner we define the 6 dB width of f_w^2 to represent the range resolution r_6. The solution of the transcendental equation for r_6 is not easy and thus we again approximate the error function by a hyperbolic tangent function. This approximation gives us an analytic solution which shows the interrelation between B_6 and τ. The solution is

$$r_6 = (1/aB_6\tau)(C\tau/2)\cosh^{-1}[2+\cosh aB_6\tau]. \quad (24)$$

The range width r_6 as a function of B_6 is shown in Fig. 4. Also shown is a numerical solution of the exact transcendental equation. We see that as the bandwidth-pulse width product gets large, the 6 dB range width approaches $C\tau/2$.

7. Signal-to-noise ratio for distributed targets

The signal-to-noise ratio for distributed targets is just simply (23) divided by kT_eB_n. Again, consistent with the above approximations, we find that S/N depends on $B_6\tau$ as

$$S/N = \frac{C_0}{r^2}[(\coth 2b) - 1/2b]\frac{\tau^2}{B_6\tau}, \quad (25)$$

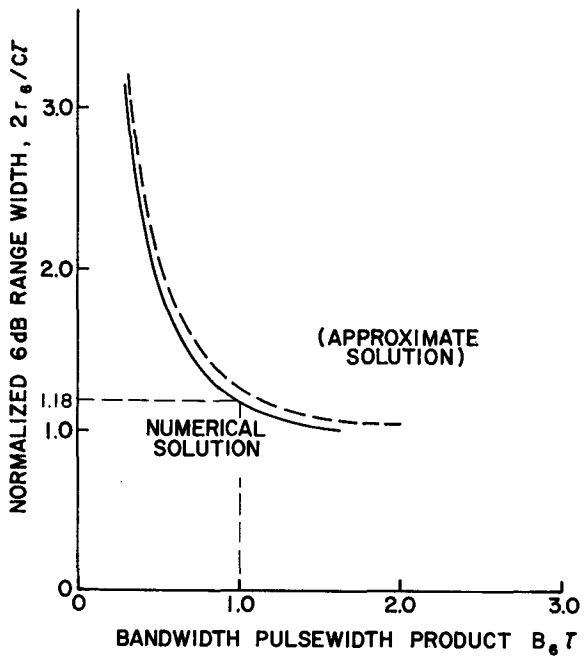

FIG. 4. Normalized 6 dB range width $2r_6/C\tau$ of the resolution volume versus receiver bandwidth-pulse width product. Numerical solution for transcendental equation is solid line and dashed line shows an approximate analytic solution given by (24).

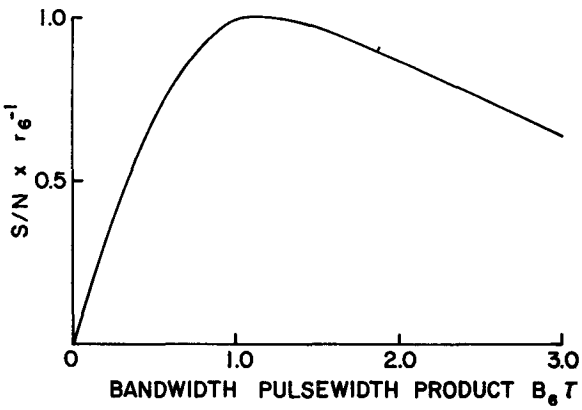

FIG. 5. Signal-to-noise ratio S/N, resolution r_6^{-1} product for distributed targets versus receiver bandwidth B_6, pulse width τ product.

where C_0 contains constants pertaining to the radar. We immediately note that if $B_6\tau$ is a constant which optimizes receiver performance, then S/N is proportional to the square of the transmitted pulse width. Also, it can be shown that maximum S/N is obtained when $B_6 \to 0$; as bandwidth decreases, both signal and noise powers are reduced, but the signal power decreases slower than noise, until in the limit S/N reaches $C_0\tau^2/3r^2$. Therefore, in contrast to point target measurements we do *not* obtain a maximum of weather S/N at $B_6\tau \approx 1$ [see Eq. (7)]. Even though S/N increases monotonically as B_6 decreases, resolution r_6^{-1} worsens. We define an optimum B_6 as that value which maximizes the product of resolution and S/N or, if r_6^{-1} is fixed, maximizes S/N. This could be a receiver design criterion for weather radar systems that Nathanson and Smith (1972) were seeking. Fig. 5 shows the dependency of the normalized product $(S/N)\times r_6^{-1}$ vs $B_6\tau$. By using this criterion, we optimize weather echo S/N at about the same $B_6\tau$ as for point target echoes. Thus we conclude that a "matched" filter receiver optimizes the distributed target signal-to-noise ratio and resolution product. A more formal derivation presented by Zrnic' and Doviak (1978) leads to the following conclusion concerning receiver design: the optimum system consists of a matched Gaussian filter and pulse which together yield the desired resolution.

8. Correlation of echo samples along range-time

Sample spacing along the range-time axis is usually chosen so that there are independent estimates of reflectivity and velocity along the beam. Both pulse width τ and receiver-filter bandwidth B_6 determine correlation of these estimates and sometimes B_6 is deliberately chosen small (i.e., not "matched" to τ) in order to observe meteorological events in a larger range interval with fewer samples along the range-time axis. This approach becomes more advantageous when real-

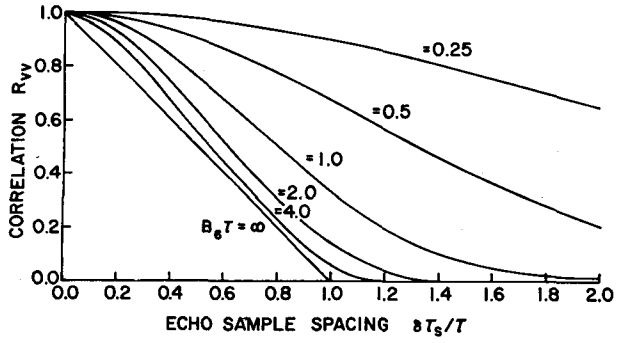

FIG. 6. Normalized correlation of echo samples spaced along the range-time axis.

time data processing equipment limits simultaneous observations to few range-time samples (as is sometimes the case for real-time Doppler spectral processors) and pulse width cannot be increased. If B_6 is "matched" to τ or, as in many meteorological radars, large compared to τ^{-1}, then dimensionally small meteorological events such as tornadic vortices can be missed by samples spaced greater than the range extent of the resolution volume. Otherwise, smaller regions need to be observed increasing the time for interrogation of the entire storm.

In this section we examine the correlation between samples along the range-time axis and determine how receiver bandwidth and transmitter pulse width affect this correlation. Sirmans and Doviak (1973) have shown that the signal at the receiver's input has a correlation R_{xx} given by

$$R_{xx}=\begin{cases}R_{xx}(0)\left[1-\dfrac{|\delta\tau_s|}{\tau}\right], & |\delta\tau_s|\leqslant\tau\\ 0, \quad \text{otherwise}\end{cases} \tag{26}$$

where $R_{xx}(0)$ is the prefilter mean power $\bar{P}(\tau_s)$. The signal $V(\tau_s)$ after passing through the filter has a correlation $R_{vv}(\delta\tau_s)$ (Papoulis, 1965, p. 346)

$$R_{vv}(\delta\tau_s)=R_{xx}(\delta\tau_s)\bigstar h^*(-\delta\tau_s)\bigstar h(\delta\tau_s), \tag{27}$$

where $h(\delta\tau_s)$ is the unit impulse response of the filter and the $\bigstar$ designates the convolution operation. For a Gaussian filter $h(\delta\tau_s)$ is given by (3) and, therefore,

$$h^*(-\delta\tau_s)\bigstar h(\delta\tau_s)\equiv\int_{-\infty}^{+\infty}h^*(-\xi)h(\delta\tau_s-\xi)d\xi$$
$$=(0.5)^2B_6(2\pi/\ln 2)^{\frac{1}{2}}\exp[-(\pi B_6\delta\tau_s)^2/8\ln 2]. \tag{28}$$

We then find the echo sample correlation R_{vv}, i.e., the convolution of the input signal correlation R_{xx} and (28),

$$R_{vv}(\delta\tau_s)=\frac{aB_6\tau\bar{P}(\tau_s)}{\sqrt{2\pi}}\int_{-1}^{+1}(1-|x|)$$
$$\times\exp[-(aB_6\tau)^2(x-\delta\tau_s/\tau)^2/2]dx. \tag{29}$$

Eq. (29) has been evaluated numerically and the results are plotted in Fig. 6. The solution shows that when B_6 is more than twice τ^{-1}, the echo sample correlation is principally controlled by pulse width, whereas when B_6 is less than $0.5\tau^{-1}$, it's controlled by the receiver-filter 6 dB bandwidth. A useful analytic formula for correlation when $B_6\ll\tau^{-1}$ is

$$R_{vv}(\delta\tau_s)=R_{vv}(0)\exp[-(aB_6\delta\tau_s)^2/2], \tag{30}$$

where $R_{vv}(0)=aB_6\tau\bar{P}(\tau_s)/\sqrt{2\pi}$.

9. Significance for Doppler velocity measurements

The optimization of pulse-Doppler radar performance is quite desirable especially when radars are used to probe clear-air mesoscale phenomena. Clear-air mapping of horizontal wind using dual-Doppler radars has been shown to be possible with moderate size weather radars (Doviak and Jobson, 1977). In this case we need to probe target ranges to at least a few tens of kilometers and sometimes beyond so that subsynoptic scales that play a role in triggering storms might be resolved.

Many weather radars transmit pulse widths of about 1 μs duration which provide a 180 m 6 dB range resolution (Fig. 4) when $B_6\tau=1$. Usually this is a finer resolution than achieved by the antenna beam at those ranges used in dual-Doppler radar synthesis of mesoscale wind. Eq. (25) shows that S/N increases as τ^2, and if range resolution is matched to angular resolution, an order of magnitude improvement in S/N might easily be obtained. However, we should not focus our attention only on S/N but on the improvement in measurement of meteorological parameters such as Doppler velocity.

Zrnic' (1977) used perturbation techniques to develop a theoretical formula for the variance in Doppler velocity determined from covariance estimation techniques. When signals are weak (i.e., $S/N\ll 1$), the variance formulas are valid (i.e., the estimator is well behaved) if (Zrnic', *op. cit.*)

$$M\gg\frac{(1+N/S)^2}{\beta^2(T_s)}, \tag{31}$$

where M is number of contiguous pairs used to estimate the signal covariance and $\beta(T_s)$ the magnitude of the signal correlation coefficient at lag T_s, the pulse repetition period. Furthermore, dwell time MT_s needs to be large compared to signal decorrelation time $\lambda/4\pi\sigma_v$, where σ_v is Doppler velocity spectrum width. Clear-air echoes have σ_v small compared to the Nyquist interval $\lambda/4T_s$ required to observe thunderstorms (Doviak, *et al.*, 1978) so $\beta^2(T_s)\approx 1$. Thus (25) and (31) show, for weak signals, that larger than an order of magnitude decrease in required M is obtained by just doubling transmitter pulse width, while maintaining matched conditions. Therefore, the dwell time $T_d=MT_s$ needed to achieve accurate velocity estimation can be decreased

by an order of magnitude, from (25) and (31):

$$T_d \gg C_1 T_s r^4 \tau^{-4}, \tag{32}$$

where the constant C_1 pertains to the radar.

However, if the radar's transmitter is average power limited, then increased pulse duration can be offset by an increase in T_s, but then signal samples are less correlated or the peak power must be reduced. Thus

$$T_d \gg \begin{cases} C_2 r^4 \tau^{-3} & \text{if } T_s \text{ is increased} \\ C_3 r^4 \tau^{-2} & \text{if peak power is reduced.} \end{cases} \tag{33}$$

Obviously the first alternative is more attractive if signal samples remain correlated; and we show, by example, how a significant decrease in dwell time results. Lower correlation tends to increase velocity estimate variance, var$[\hat{V}]$, as can be seen from the formula (Zrnic', 1977)

$$\text{var}[\hat{V}] = \frac{\lambda^2 e^{(4\pi\sigma_v T_s/\lambda)^2}}{32\pi^2 M T_s^2} \times \left\{ \left(\frac{N}{S}\right)^2 + 4\left(\frac{N}{S}\right)\left(\frac{4\pi\sigma_v T_s}{\lambda}\right)^2 + \frac{4\pi^3 \sigma_v T_s}{\lambda} \right\}. \tag{34}$$

This formula is exact to first order in M and does not require $\beta^2(T_s)$ to be near unity, but (31) must hold. We now consider a signal spectrum width σ_v of 2 m s^{-1}, $T_s = 10^{-3}$ s, $\lambda = 0.1$ m and an echo that produces $N/S \approx 10$. The dwell time T_d required to generate a var$[\hat{V}] = 1$ m^2 s^{-2} is [from (34)] 3.5 s. However, if pulse width is tripled so that N/S is decreased to about unity and T_s is tripled to maintain constant average transmitted power, the dwell time needed to produce an equivalent var$[\hat{V}]$ is now 0.1 s, a decrease larger than a factor of 30.

Something else must be considered—this is the range correlation of echo samples. As $B_6\tau$ increases (Fig. 6), equally spaced echo samples become more correlated and thus we lose velocity variance reduction that could be achieved by averaging echo samples spaced apart at lags equal to the shorter pulse width. In our example we lose a factor of about 3 in the decrease of var$[\hat{V}]$ so that the net decrease in T_d for this case is about 10, still a significant reduction.

If σ_v remains sufficiently small so that (34) is well approximated by

$$\text{var}[\hat{V}] \approx \frac{\lambda^2}{32\pi^2 M T_s^2}\left(\frac{N}{S}\right)^2, \tag{35}$$

it is easily seen (when both average transmitter power and dwell time $T_s M$ are constrained) that velocity estimate variance decreases by the 5th power of τ! Here again we lose variance reduction because we have less independent velocity estimates along range if τ is increased. The net result is that var$[\hat{V}]$ can be reduced by τ^{-4}, a considerable reduction.

The conditions (i.e., S/N, σ_v) cited above are those which may occur when moderately sensitive dual-Doppler radars sense clear air at ranges necessary to map mesoscale velocity fields. This is the experience gained at NSSL from a few experiments conducted during our severe storm season.

10. Summary and conclusions

Loss L_r in weather echo signal strength due to finite receiver bandwidth was first examined by Nathanson and Smith (1972) who considered an ideal matched filter receiver and deduced L_r to be 1.8 dB. We have herein cast the problem in a general form and assumed a realistic receiver transfer characteristic. For conditions $B_6\tau = 1$, a Gaussian filter and rectangular transmitted pulse we find $L_r \approx 2.3$ dB. Fig. 3 shows the L_r dependence on $B_6\tau$.

It is demonstrated that the correlation along the range-time axis depends on the receiver filter bandwidth and transmitted pulse width (Fig. 6). For receivers with large bandwidths compared to the reciprocal of pulse width, this correlation is a function of the transmitted pulse shape alone. Narrower bandwidths increase considerably the correlation time along the range-time axis.

Considerable improvement in radar signal detection can often be obtained by using a matched filter receiver and pulse width giving a range resolution nearly equal to the angular one determined by the antenna. It is shown, by way of example, that an order-of-magnitude improvement in system performance can often be achieved when range width r_6 is matched to beamwidth $r\phi_1$ at those ranges required to map mesoscale wind.

We recommend use of the weather radar equation derived herein because it does explicitly show losses due to finite receiver bandwidth and the atmosphere, both of which can be significant. At centimeter wavelengths, atmospheric losses should not be neglected even in the clear air (Blake, 1970).

Acknowledgments. The authors express their appreciation to Mr. W. Bumgarner for numerical solutions and Mr. A. Zahrai for manuscript review. We also thank Ms. Jennifer Moore for preparing the figures and Mr. C. Clark for his photographic services. Special thanks to Ms. Joy Walton for her efficient and accurate typing, and careful preparation of the manuscript. This work was partially supported by FAA Contract DOT-FA76-WAI-622.

REFERENCES

Abramowitz, M., and I. A. Stegun, 1964: *Handbook of Mathematical Functions*. Nat. Bur. Stnds., *Appl. Math. Ser.*, No. 55, 1046 pp. [Govt. Printing Office].

Atlas, D., 1964: Advances in radar meteorology. *Advances in Geophysics*, H. E. Landsberg and J. Van Mieghem, Eds., Academic Press, 317–478.

Blake, L. V., 1970: Prediction of radar range. *Radar Handbook*, Merrill I. Skolnik, Ed., McGraw-Hill, 1–73.

——, and C. T. Jobson, 1977: Mapping clear air winds with dual Doppler radars. *Proc. Int. Symp. EM Wave Propagation in Non-ionized Media*, LaBaule, France, Edité pour le Centre National d'Études des Telecommunications, 505–510.

Doviak, R. J., and C. T. Jobson, 1977: Mapping clear air winds with dual Doppler radars. *Proc. Int. Symp. EM Wave Propagation in Non-ionized Media*, LaBaule, France, Edité pour le Centre National d'Études des Telecommunications, 505–510.

——, D. Sirmans, D. Zrnic′ and G. B. Walker, 1978: Considerations for pulse-Doppler radar observations of severe thunderstorms. *J. Appl. Meteor.*, **17**, 189–205.

Hennington, L., R. J. Doviak, D. Sirmans, D. Zrnic′ and R. G. Strauch, 1976: Measurement of winds in the optically clear air with microwave pulse-Doppler radar. *Preprints 17th Conf. Radar Meteorology*, Seattle, Amer. Meteor. Soc., 342–348.

Nathanson, F. E., 1969: *Radar Design Principles*. McGraw-Hill 227–283.

——, and P. L. Smith, 1972: A modified coefficient for the weather radar equation. *Preprints 15th Radar Meteorology Conf.*, Champaign-Urbana, Amer. Meteor. Soc., 228–230.

Papoulis, A., 1965: *Probability Random Variables and Stochastic Processes*. McGraw-Hill, 346 pp.

Probert-Jones, J. R., 1962: The radar equation in meteorology. *Quart. J. Roy. Meteor. Soc.*, **88**, 485–495.

Sirmans, D., and R. J. Doviak, 1973: Meteorological radar signal intensity estimation. NOAA Tech. Memo ERL NSSL-64, 69–71.

Taylor, J. W., and J. Mattern, 1970: Receivers. *Radar Handbook*, Merrill I. Skolnik, Ed., McGraw-Hill, 1–50.

Zrnic′, D., 1977: Spectral moment estimates from correlated pulse pairs. *IEEE Trans. Aerospace Electron. Sys.*, **AES-13**, 344–354.

——, and R. J. Doviak, 1978: Matched filter criteria and range weighting for weather radar. *IEEE Trans. Aerospace Electron. Syst.* (in press).